



Mammalian Expression and Biophysical Examination of Human Wild Type Optineurin Protein

Hongyu Ying, Xiang Shen, Minhua Wang, Beatrice Y.J.T. Yue.

Department of Ophthalmology and Visual Sciences, College of Medicine, University of Illinois at Chicago, Chicago, Illinois, USA.

1. Abstract

The optineurin gene has been linked to normal tension glaucoma and amyotrophic lateral sclerosis. Optineurin protein, known to interact with a number of proteins including Rab8, myosin VI, and huntingtin, plays a role in vesicle trafficking, Golgi organization, antibacterial and antiviral signaling, autophagic clearance of protein aggregates, and regulation of gene expression. Its basic biophysical properties however have never been explored. This study was aimed to obtain sufficient amounts of purified mammalian optineurin protein and to carry out biophysical characterization. Tetracycline inducible RGC-5 cell line that expresses Halo tagged human wild type optineurin was created. Tag free optineurin was purified and its purity was assessed by SDS-PAGE and Western blotting. The secondary structure of the highly purified optineurin was examined by circular dichroism (CD) spectropolarimeter. The posttranslational modification sites were identified by liquid chromatography-mass spectrometry. Protein-protein interaction was evaluated by bimolecular fluorescence complementation (BiFc) analysis. The aggregation of optineurin was studied by thioflavin T (ThT) assay. The CD spectra indicated that the tag free optineurin protein was folded, containing both α -helical and β -sheet secondary structures. One previously reported phosphorylation site serine (Ser) 177, four novel phosphorylation sites (Ser173, 174, 526 and 528), as well as one new acetylation site (Ser2) were identified. Optineurin protein was also shown to be an aggregate prone protein. It interacted with itself as detected by BiFc assay, and formed β -sheet rich structures or aggregates as evidenced by ThT assay.

Keywords: Human optineurin protein; Mammalian expression; Tet-on inducible cell line; Posttranslational modification sites; Circular dichroism; Bimolecular fluorescence complementation (BiFc); Thioflavin T (ThT) assay.

2. Introduction

The optineurin gene was originally identified through a yeast two-hybrid screening by Li et al. [1] using an adenovirus protein E3-14.7K (group C early transcription region 3 14.7-kDa protein) as a bait and was initially named as FIP-2 (14.7K-interacting protein 2). E3-14.7K protein inhibited tumor necrosis factor- α (TNF- α) induced apoptosis and FIP-2 could reverse such an effect in human 293 cells [1]. The protein was subsequently noted to display a high homology with NF- κ B essential molecule (NEMO), and was named NRP (NEMO related protein) [2]. In 2002, this gene was identified as a causative gene on chromosome 10p14 in a study of 54 families with autosomal dominantly inherited adult-onset primary open angle glaucoma (POAG) and was designated as "optic neuropathy inducing" or optineurin [3]. It was further noted that variations in this gene predominantly resulted in normal tension glaucoma, a subtype of POAG [3]. More recently, optineurin gene has also been linked to amyotrophic lateral sclerosis (ALS) [4-6].

Optineurin, a 67-kDa protein, is expressed in most tissues such as the heart, brain, placenta, skeletal muscle, kidney, pancreas, liver, and the eye [3, 7]. The putative domains in optineurin protein include: a NEMO-like domain, at least one leucine zipper, multiple coiled-coil motifs, an ubiquitin-binding domain (UBD), a microtubule associated protein 1 light chain 3 (LC3)-interacting motif [8], and a carboxyl (C)-terminal C2H2 type of zinc finger [1, 2, 9-11]. The endogenous or ectopically expressed optineurin has been shown to interact with itself to form high molecular weight protein complexes (HMCs or homo-oligomer) in RGC-5 [12], NIH3T3 [13] and 293T [2, 13] cells. It also binds with other proteins such as Rab8 [14, 15], huntingtin [16], myosin VI [17], transferrin receptor [18, 19], metabotropic glutamate

receptor [20], LC3 [8], polo-like kinase 1 (Plk1) [21], and TANK (TRAF-associated NF- κ B activator) binding kinase 1 (TBK1) [8, 22]. These interactions depict basic optineurin functions or participation in cellular processes including vesicle trafficking [18, 19, 23], maintenance of the Golgi apparatus [24, 25], NF- κ B pathway [26-30], anti-bacterial [8] and anti-viral signaling [28], cell division control [21], and autophagy [31-33]. Optineurin has in addition been shown to be phosphorylated, which is essential for its functions in mitosis [21] and autophagic signaling pathway [8, 33, 34].

Despite intense interests and extensive studies on optineurin in the past decade, its biophysical properties and/or three dimensional structure have yet to be explored. The effort has been hampered largely by challenges of accessing sufficient amounts of purified mammalian optineurin protein. In this report, we described the establishment of stable inducible tetracycline regulated (Tet-on) optineurin-Halo expressing RGC-5 cell lines and the purification of tag free human optineurin protein using the Promega's HaloTag based purification technique. The stable cell lines which express optineurin upon doxycycline (Dox) induction provide an excellent source to produce highly purified recombinant protein for biophysical characterization including its secondary structure, phosphorylation sites, and aggregation as shown herein. Oligomer/dimer formation was also examined by the bimolecular fluorescence complementation (BiFC) assay which is based on the principle that two non-fluorescent N- and C-terminal fragments of a fluorescent protein such as green fluorescent protein (GFP) can re-associate and form a fluorescent complex when they are fused to two proteins that interact with each other or one protein such as α -synuclein that forms dimers/oligomers [35, 36].

3. Methodology

The study did not use animals or involve human subjects. Experiments were carried out using RGC-5 and mouse neuroblastoma Neuro2A cell lines.

3.1. Plasmids

Plasmid pTRE-OPTN_{WT}-Halo-IRES-GFP-INS-CMVp-rtTA-IRES-Hyg was made in several steps. Human wild type full length optineurin (OPTN) gene PCR amplified from plasmid pOPTN_{WT}-EGFP [24] was subcloned into Halo expression vector pFC14K-CMV (Promega, Madison, WI, USA) to create pOPTN_{WT}-Halo. Tetracycline regulated expression vector pTRE-OPTN_{WT}-Halo-IRES-GFP-INS-CMVp-rtTA-IRES-Hyg was constructed using MultiSite Gateway Pro 4.0 System from Invitrogen (Grand Island, NY, USA) by four pieces recombination of entry vectors with destination vector. Briefly, entry vector containing TRE promoter (pENTR L1-TRE-L5r) was made by PCR amplification of attB1-attB5 flanked TRE and recombined with donor vector pDONR 211 P1-P5r. Entry vectors containing OPTN_{WT}-Halo (pENTR L5-OPTN_{WT}-Halo-L4), IRES-GFP (pENTR L4r-IRES-GFP-L3r) and INS (pENTR L3-INS-L2) were similarly made. Destination vector containing pCMVp-rtTA-IRES-Hyg was made by insertion of rfa element (destination conversion system from Invitrogen) into pCMVp-rtTA-IRES-Hyg-pcDNA3.1z [37]. Finally LR reaction was performed using four entry vectors pENTR L1-TRE-L5r, pENTR L5-OPTN_{WT}-Halo-L4, pENTR L4r-IRES-GFP-L3r, pENTR L3-INS-L2 and destination vector pCMVp-rtTA-IRES-Hyg-rfa to generate plasmid pTRE-OPTN_{WT}-Halo-IRES-GFP-INS-CMVp-rtTA-IRES-Hyg.

For BiFC analysis, pOPTNWT-YN, pYN-OPTN_{WT}, and pOPTNWT-YC, were constructed using Gateway Multisite pro 4.0 System (Invitrogen). Full length optineurin gene was subcloned into pDONR 211 P1-P5r to produce entry vector pENTR L1-OPTNWT-L5r. YN (1-154 amino acids of enhanced yellow fluorescent protein or EYFP) was PCR amplified from bJun-YN (courtesy of Dr. Tom Kerppola) [38] and subcloned into pDONR 211 P5-P2 to make pENTR L5-YN-L2. LR reaction of these two entry vectors pENTR L1-OPTN-L5r and pENTR L5-YN-L2, and destination vector pCMV/Zeo (Promega) was performed to make plasmid pOPTNWT-YN. pYN-OPTNWT was generated by a similar strategy. A YN fluorescent complementary YC plasmid pOPTNWT-YC was also generated. YC (155-238 amino acids of EYFP) was PCR amplified from bFos-YC (courtesy of Dr. Tom Kerppola) [38] and subcloned into pDONR 211 P1-P5r to generate pENTR L1-YC-L5r, and OPTNWT was subcloned into pDONR 211 P5-P2 to generate pENTR L5-OPTN-L2. LR recombination was performed using pENTRL1-OPTN-L5r, pENTR L5-YC-L2 and destination vector pCMV/Zeo to generate pOPTNWT-YC. All plasmids were sequenced to verify the sequence integrity and in frame fusion of genes.

3.2. Establishment of Tet-on Wild Type Optineurin-Halo Expressing Stable RGC-5 Cells

RGC-5 cells were transiently transfected for 20 h with plasmid pTRE-OPTN_{WT}-Halo-IRES-GFP-INS-CMVp-rtTA-IRES-Hyg in T-25 flasks using Lipofectamine LTX transfection reagent (Invitrogen). The complete growth medium (Dulbecco's Modified Eagle's medium or DMEM with 10% fetal bovine serum) was changed to selection medium containing 100 μ g/ml of hygromycin (EMD Millipore, Billerica, MA, USA) and the selection continued for about 2 weeks until medium sized colonies grew out. The cells were then trypsinized and induced with 1 μ g/ml of Dox (Clontech, Mountain View, CA, USA) for 24 h. GFP-expressing or GFP positive cells were sorted using DakoCytomation MoFlo into 96 well plates (1 cell/well) with maintenance medium (with 50 μ g/ml of hygromycin but without Dox) for another 2 weeks. Cells were screened for GFP expression after induction with Dox by fluorescence microscopy. Bright GFP positive clones (high expresser clones) were allowed to multiply and were banked in liquid nitrogen.

3.3. Purification of Tag Free Optineurin Protein

Tet-on optineurin-Halo inducible RGC-5 cells were induced with complete medium plus Dox (1 µg/ml) for 24 h. Cells were lysed in 50 mM Tris-HCl, 150 mM NaCl, supplemented with 0.005% NP40 and proteinase inhibitor, pH 7.4 and purified using Promega's HaloTag based affinity purification technique under native conditions. Briefly, total lysate was incubated with HaloLink resin overnight at 4°C. The resin was subsequently washed three times with lysis buffer, and the protein on the beads was incubated overnight at 4°C with Halo-TEV protease in washing buffer (same as lysis buffer). Tag free optineurin protein was collected the next day following centrifuging at 5,000 rpm for 5 min (referred to as elute 1). The beads were incubated with lysis buffer again for elutes 2 and 3. The purity of the isolated protein was assessed by SDS-PAGE and Coomassie blue staining.

For purification of phosphorylated optineurin protein, NaCl in the lysis buffer was replaced with same concentration of NaF, a potent phosphatase inhibitor.

3.4. Western Blotting

Samples from different stages of the purification process were resolved on 10% SDS-PAGE gels and transferred to nitrocellulose membrane. The membrane was immunoblotted with anti-optineurin polyclonal antibody (Cayman Chemical, Ann Arbor, MI, USA). To examine whether the purified optineurin protein was phosphorylated, the protein was immunoblotted with anti-phosphotyrosine and anti-phosphoserine monoclonal antibodies (Sigma, St. Louis, MO, USA).

3.5. Liquid Chromatography-Mass Spectrometry (LC-MS/MS) Analysis

Posttranslational modification sites of optineurin protein were identified by LC-MS/MS at the Mass spectrometry, Metabolomics & Proteomics Facility, Research Resources Center, University of Illinois at Chicago. Briefly, purified optineurin protein was digested with trypsin (Promega), and phosphorylated peptides were enriched using NTA medium (Qiagen, Germantown, MD, USA). Both the retained and the unretained fractions were subjected to nano scale LC/MS/MS analysis on a LTQ Orbitrap Velos Pro mass spectrometer (Thermo Scientific, Waltham, MA, USA). Raw data acquisition files were processed with the Mass Matrix File Conversion tool to generate Mascot generic files and searched against NCBI database. The variable modifications include: phosphoserine (pSer), threonine (pThr) and tyrosine (pTyr) as well as acetylation at the N-terminus of the protein.

3.6. Circular Dichroism (CD) Spectroscopy

CD spectra of purified optineurin at 0.03 mg/ml in 50 mM Tris, 150 mM NaF, pH 7.4 were collected using a Jasco J-710 CD spectrometer at room temperature with a 2 mm path length cuvette [39]. Deconvolution was performed utilizing Dichroweb (<http://dichroweb.cryst.bbk.ac.uk/html/home.shtml>) using a mean residue molecular weight of 115 [40].

3.7. BiFc Assay

Mouse neuroblastoma Neuro2A cells plated into Lab-Tek II CC2 8-well chamber slides (10,000 cells/well) were cultured overnight. The cells were co-transfected for 20 h with combinations of BiFc plasmids (pOPTN-YN + pOPTN-YC; pYN-OPTN + pOPTN-YC; pbJun-YN + pbFos-YC) using lipofectamine LTX, fixed with 4% paraformaldehyde and mounted with Vectashield with 4',6-diamidino-2-phenylindole (DAPI) (Vector Laboratory, Burlingame, CA, USA). Images were taken on Zeiss LSM-710 confocal microscope (Carl Zeiss, Thornwood, NY, USA) using a GFP filter. The fluorescence observed was thus green (GFP) rather than yellow (YFP). Cells transfected with pOPTN-YN or pOPTN-YC alone were used as negative control while co-transfected with pbJun-YN + pbFos-YC were served as positive control.

3.8. Thioflavin T (ThT) Assay

The aggregation or fibril formation of optineurin was examined by ThT assay. Purified optineurin diluted in 50 mM Tris-HCl, 150 mM NaCl, pH 7.4 was incubated at 37°C for up to 4 days. ThT (Sigma) solution was added (10 µM in 50 mM glycine-NaOH, pH 8.5) into each tube, mixed by vortex and transferred into black 96-well polystyrene plates. Fluorescence was read on TECAN GENios pro plate reader (TECAN, Salzburg, Austria). The excitation wavelength used was 450 nm, and the emission wavelength was 485 nm. All assays were performed in triplicate. For the effect of different ionic strength on the aggregation/fibril formation, purified optineurin was incubated at 37°C for 4 days in 50 mM Tris, pH 7.4 containing 0-2 M of NaCl.

4. Results

4.1. Purification of Tag Free Human Optineurin Protein

Inducible Tet-on optineurin-Halo expressing RGC-5 stable cell line was established using a single plasmid vector pTRE-OPTN-Halo-IRES-GFP-INS-CMVp-rtTA-IRES-hyg-pcDNA3.1z (**Figure 1**) which contains both tetracycline regulatory

and responsive components based on Clontech's Tet-on advance system. Optineurin-Halo was expressed along with GFP when the cells were induced with Dox (1 $\mu\text{g}/\text{ml}$) for 24 h (Figure 2).

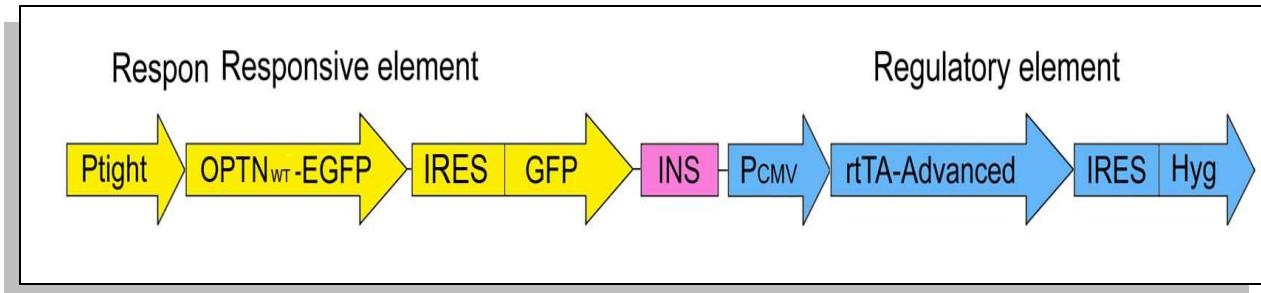


Figure 1. Schematic presentation of single plasmid construct used to make Tet-on inducible human optineurin-Halo (OPTN_{WT}-Halo or OPTN-Halo) expressing RGC-5 stable cell line. There are two expression cassettes in this plasmid. In responsive element expression cassette (yellow), OPTN-Halo and IRES-GFP are under the control of Ptight promoter and in regulatory element expression cassette (blue), rtTA-Advance and IRES-hygromycin (IRES-Hyg) are under the control of CMV promoter. These two expression cassettes are separated by 5'-HS4 chicken β -globin insulator (INS, in pink).

The human optineurin protein expressed was purified and isolated with high purity (Figure 3A) using Halo purification strategy from Promega. Optineurin-Halo fusion protein has a molecular weight of around 100 kDa. After cleavage by Halo-TEV (Halo-tagged TEV protease, which is the 27 kDa catalytic domain of the nuclear inclusion a protein encoded by tobacco etch virus), the tag free optineurin was eluted with molecular weight of around 74 kDa. On the SDS gel, there was also a faint band with a molecular weight slightly higher than the optineurin band which might represent phosphorylated optineurin (Figure 3A).

Western blotting using rabbit anti-C-terminal optineurin indicated that the elutes after TEV digestion were tag free optineurin (Figure 3B). With a modified protocol in which NaCl in the lysis buffer was replaced with NaF, a general inhibitor for protein phosphatases, the higher molecular weight band in the doublet (phosphorylated optineurin population) was dramatically enhanced (Figure 3C). Both bands of the doublet were sent for mass spectrometry and were verified to be human optineurin protein (Figure 4A). Immunoblotting further showed that the purified optineurin, immunoreactive to both anti-phosphotyrosine and anti-phosphoserine monoclonal antibodies, was tyrosine- and serine-phosphorylated (Figure 3D), as was the endogenous optineurin demonstrated previously [12]. The yield of highly purified optineurin protein was approximately 23 $\mu\text{g}/500 \text{ cm}^2$ dish.

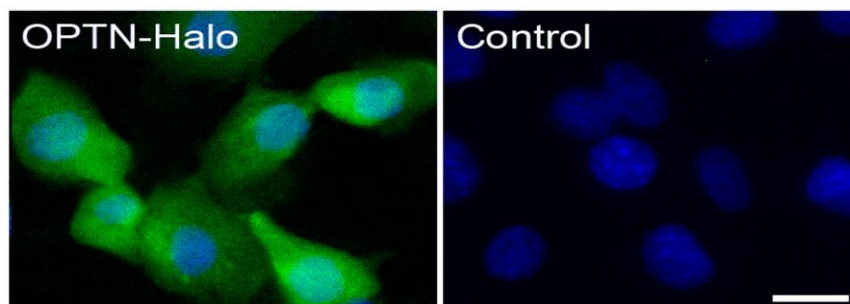


Figure 2. Expression of optineurin-Halo in Tet-on inducible RGC-5 stable cells. A representative clone (OPTN-Halo) showed GFP expression (from IRES-GFP, see Figure 1) after Dox (1 $\mu\text{g}/\text{ml}$) induction for 24 h. The same clone showed minimal green fluorescence in growth medium without Dox (Control). This indicates the human OPTN-Halo fusion gene expression under Dox induction but no such an expression without induction. The nuclei were stained with DAPI in blue. Scale bar, 20 μm .

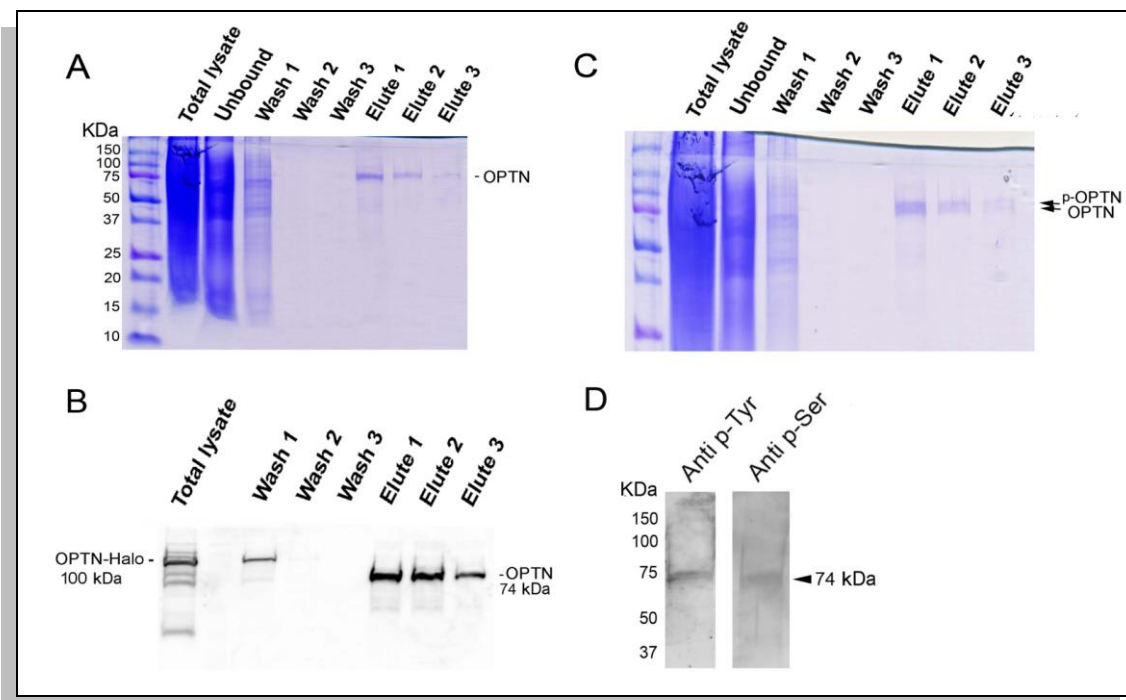


Figure 3. Purification of tag free human optineurin (OPTN) protein. Samples from different stages of the purification process were resolved on 10% SDS-PAGE gels. The gels were either stained with Coomassie blue (A) or immunoblotted with rabbit anti-optineurin (C-term) polyclonal antibody for Western blot analyses (B). The molecular weight of optineurin-Halo is about 100 kDa and that of the tag free optineurin is 74 kDa. The purified tag free optineurin was seen in elutes 1, 2, and 3. C. Phosphorylated optineurin (pOPTN) was enriched using a modified purification procedure. D. Phosphorylated optineurin reacted with anti-phosphotyrosine (Anti p-Tyr) and anti-phosphoserine (Anti p-Ser) indicating that the purified optineurin was tyrosine- and serine-phosphorylated.

4.2. Identification of Posttranslational Modification Sites

The purified optineurin protein (both unphosphorylated and phosphorylated) was trypsin digested. Phosphopeptides were further enriched by passing through a phosphopeptide enrichment column. When subjected to LC-MS/MS analysis, the spectra showed a 43% amino acid sequence coverage (Figure 4A). Five phosphorylated serine sites: Ser173, 174, 177, 526, and 528 were identified (Figure 4B). Ser2 was also found to be acetylated (Figure 4B). Representative spectra of phosphorylation at Ser174 and 177 are shown in Figure 4C and D.

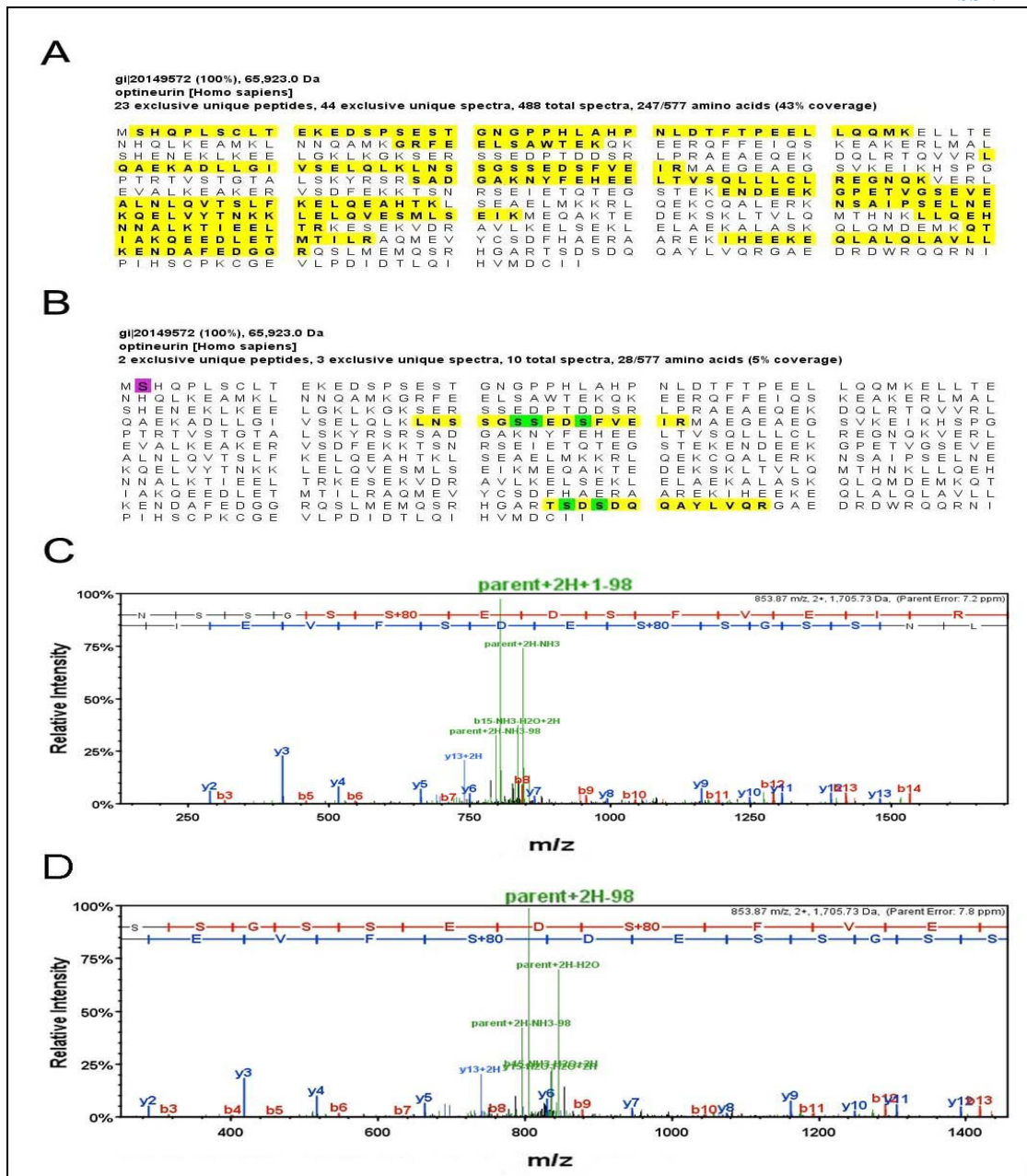


Figure 4. A. Identification of human optineurin by mass spectrometry. Purified optineurin gel bands (doublet) were analyzed by mass spectrometry and were identified to be human optineurin protein. 23 exclusive unique peptides were identified that covered 43% of total optineurin amino acids (highlighted in yellow). **B.** Posttranslational modifications of amino acids such as phosphorylation (highlighted in green) and acetylation (highlighted in purple) were found. **C.** Representative spectra of phosphorylation at Ser174. **D.** Representative spectra of phosphorylation at Ser177.

4.3. Secondary Structure of Optineurin Protein

CD spectroscopy was carried out to test whether the purified optineurin was in fact folded and to examine its secondary structure. As shown in **Figure 5**, optineurin adopted a folded conformation containing α -helix and β -strand elements as expected. Deconvolution of the data estimated that the helix content was 30%, β -strand content was 18%, turn content was 16%, and unordered was 36%. This indicated that optineurin was mostly α -helix and unordered, suggesting that the protein might be highly flexible, or possibly consisted of largely of helical domains separated by flexible linker regions.

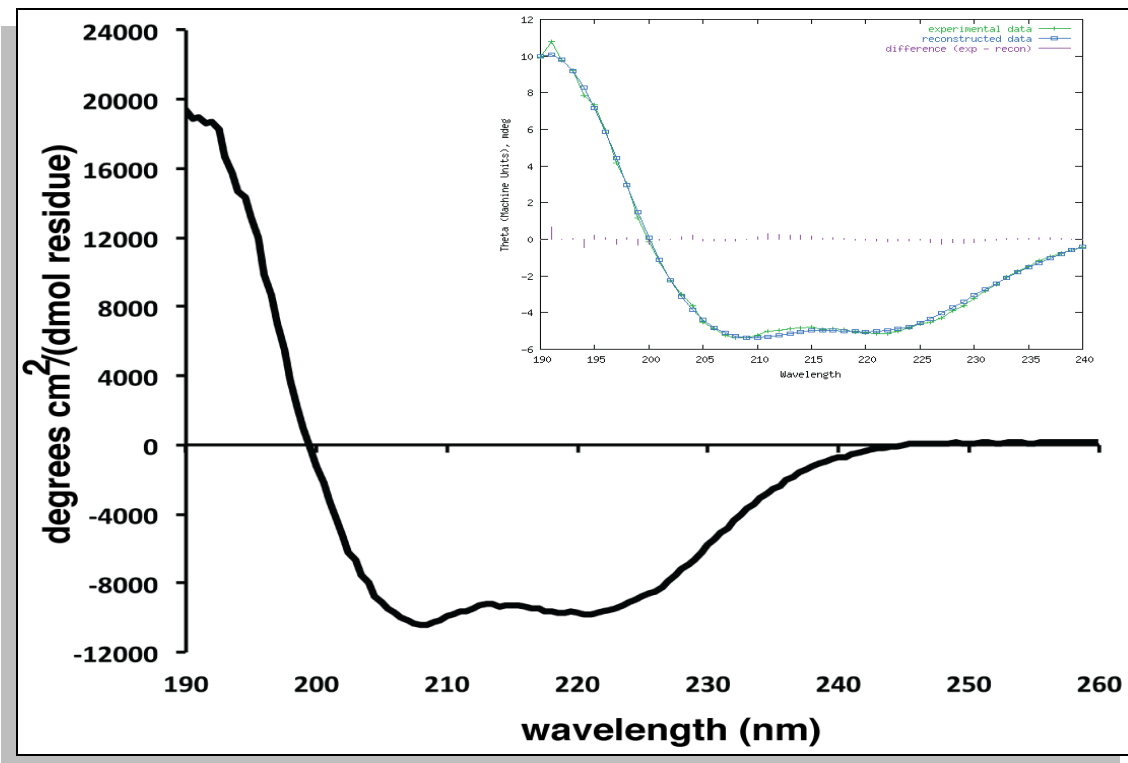


Figure 5. Circular dichroism spectrum of purified optineurin. The spectrum indicates that purified optineurin adopts a folded conformation, containing both α -helix and β -strand secondary structure. The data is displayed as mean residue ellipticity. The inlay represents the fit of the deconvoluted data using Dicroweb. The estimated helix content is 30%, β -strand content is 18%, turn content is 16%, and unordered is 36%.

4.4. BiFc Assay

BiFc plasmids pair pOPTN-YN + pOPTN-YC, pYN-OPTN + pOPTN-YC, or pbJun-YN + pbFos-YC (positive control) were co-transfected into Neuro2A cells. Transfection with single plasmid pOPTN-YC or pOPTN-YN, which was served as negative control, did not generate any fluorescence in the cells (Figure 6A). By contrast, fluorescence was observed (Figure 6C and D) in the cytoplasm of cells with pOPTN-YN + pOPTN-YC or pYN-OPTN + pOPTN-YC co-expression. The N- and C-terminal EYFP fragments would be brought together to constitute fluorescence only if and when optineurin protein interacted with itself to form dimers/oligomers. The positive result thus signified the dimer/oligomer formation by optineurin in cells. The binding of bJun and bFos (positive control) also led to fluorescence in the nuclei of cells as anticipated (Figure 6B).

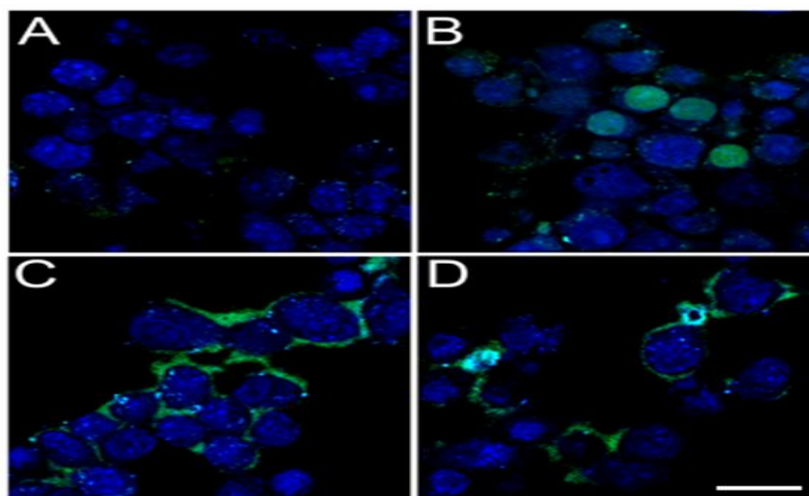


Figure 6. Protein-protein interaction assayed by BiFc. Neuro2A cells were transfected for 20 h with A. pOPTN-YN or pOPTN-YC plasmid only to serve as negative control; B. pb-Jun-YN + pb-Fos-YC to serve as positive control; C. pOPTN-YN + pOPTN-YC; and D. pYN- OPTN + pOPTN-YC. Images were examined under a Zeiss confocal microscope using a GFP filter. No fluorescence was seen in the negative control group (A), while it was observed in the nuclei in the positive control (B). Fluorescence was also detected in the cytoplasm in the pOPTN-YN + pOPTN-YC (C) and pYN-OPTN + pOPTN-YC (D) co-transfection groups indicating homo-dimerization or oligomerization between optineurin molecules. Nuclei were stained with DAPI. Scale bar, 20 μ m.

4.5. ThT Assay

Protein aggregation and fibril formation was examined by ThT assay. Purified optineurin protein incubated in physiological buffer (50 mM Tris-HCl, 150 mM NaCl, pH7.4) resulted in a heightened ThT fluorescence intensity, which was increased with the incubation time (**Figure 7A**). Bovine serum albumin, under the same conditions, showed minimal effect. The increase of ThT fluorescence by optineurin protein was also observed with increased ionic strength from 0.15 M to 2M NaCl in 50 mM Tris-HCl, pH 7.4 buffer (**Figure 7B**).

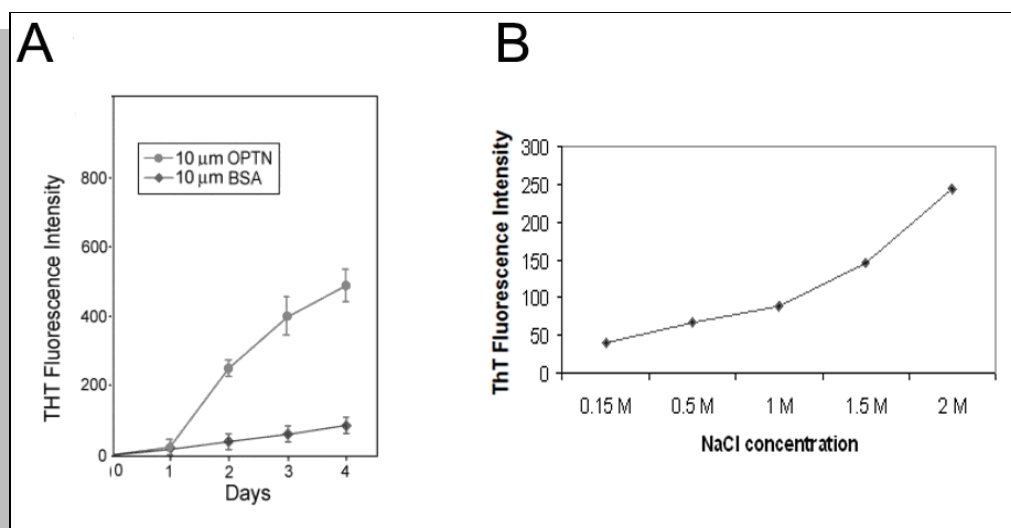


Figure 7. A. ThT emission intensity for 10 μ M of purified optineurin (OPTN) and bovine serum albumin (BSA, negative control). All were incubated at 37°C in 50 mM Tris-HCl, 150 mM NaCl (pH 7.4) for 1-4 days. **B.** ThT emission intensity for 1.5 μ M of purified optineurin in 50 mM Tris-HCl (pH 7.4) with various ionic strengths (0.15 M, 0.5 M, 1 M, 1.5 M, or 2 M NaCl). Protein was incubated at 37°C for 4 days.

5. Discussion

Optineurin has raised high interests in recent years due to its association with neurodegenerative diseases [41, 42] such as normal tension glaucoma [3, 43, 44] and ALS [45, 46]. To facilitate biophysical characterization, Halo tagged optineurin was expressed in the current study under native condition in mammalian cells and tag free optineurin was purified via Promega's Halo technology. As optineurin overexpression following a 48 h transient transfection has been shown to be toxic [24], a tetracycline regulated Tet-on inducible RGC-5 cell line was established to express human optineurin-Halo fusion protein. RGC-5 was originally created as a rat retinal ganglion cell line, however it was re-characterized recently to be, in fact, a mouse 661W photoreceptor cell line [47-49]. This cell line nevertheless was used in the present report simply as a "factory" to produce optineurin protein, not as a model for retinal ganglion cells. HaloTag is a modified haloalkane dehalogenase found only in certain bacteria. The binding of Halo tag to the HaloLink resin is covalent and essentially irreversible; it overcomes the equilibrium-based binding limitations associated with affinity tags and enables efficient capture and purification of target protein, even at low expression levels [50]. Another advantage to use Halo tag is that the target protein is released from the HaloLink resin by specific cleavage using a TEV protease fused to Halo tag (Halo-TEV), leaving both Halo tag and Halo-TEV permanently attached to the resin and highly pure, tag free protein in solution. Through this technology, we were able to obtain tag free, properly folded (**Figure 5**) optineurin protein with high purity (**Figure 3A**) in high yield. To our knowledge, this is the first time that mammalian optineurin was purified in native conditions. The inducible cell line would provide a reliable source for highly purified recombinant protein in a scaled-up and cost-effective manner for biophysical studies of optineurin.

Using LC-MS/MS, five phosphorylated serine sites in optineurin (Ser173, 174, 177, 526 and 528) were identified (**Figure 4B**). Ser177 has been reported previously that it can be directly phosphorylated by polo-like kinase 1 (Plk1) [21] or TANK-binding kinase 1 (TBK1) [8]. Plk1 belongs to a conserved subfamily of serine/threonine protein kinases that have pivotal roles in the cell-cycle progression [51]. Following phosphorylation at Ser177 by Plk1, optineurin is shown to associate with a myosin phosphatase complex, which antagonizes the mitotic activity of plk1 [21]. TBK1 is a NF- κ B-activating serine/threonine kinase that has important roles in multiple signaling pathways such as innate immunity, autophagy, and cancer [52]. TBK1 is documented to phosphorylate optineurin also at Ser177, enhancing thereby the binding affinity of optineurin to LC3 and the autophagic clearance of cytosolic Salmonella enteric through an ubiquitin-dependent pathway [8]. Phosphorylation of optineurin at Ser177 by TBK1 in addition can regulate clearance of protein aggregates via an ubiquitin-independent autophagy pathway [53].

Interestingly, Wild et al. [8] speculated that a stretch of serines (169N**SSGSSEDS**FVEIRMA184) in the LIR motif of optineurin might be phosphorylated. We herein provide direct evidence that Ser173, 174, 177 are phosphorylated in this region and suggest that the multiple serine phosphorylation sites may be crucial for optineurin's physiological function. Furthermore, we found two additional novel phosphorylation sites at Ser526 and 528 which are close to the C-terminus of the optineurin protein. The serine phosphorylation at the C-terminus is likely also of importance in optineurin's function.

The purified optineurin protein did exhibit reactivity toward anti-phosphotyrosine (**Figure 3D**). However, LC-MS/MS failed to detect any tyrosine phosphorylation site for optineurin. Increasing the coverage of peptides in the LC-MS/MS analyses may help to identify phosphorylation sites on optineurin in the future.

Ser2 was found to be acetylated (**Figure 4B**) by LC-MS/MS. A majority of eukaryotic proteins are subjected to N-terminal acetylation which emerges as a multifunctional regulator, acting as a protein degradation signal, an inhibitor of endoplasmic reticulum translocation, and a mediator of protein complex formation [54]. The finding of a new acetylation site in optineurin is of interest although its significance is unclear at present.

The CD result (**Figure 5**) indicates that optineurin protein is folded, consisting of both α -helix and β -strand elements. The protein appears to be highly flexible, possibly containing helical domains separated by flexible linker regions. The structural flexibility may be the basis why optineurin can interact with quite a few proteins and function in multiple cellular pathways. It is believed that optineurin, via different sequence regions, can impact biologic processes through protein interactions and exert different functions. Mutations or truncations in specific regions may lead to the development of pathogenic consequences. Detailed illustration and verification in this regard however must await X-ray crystallography work for the high resolution 3-dimensional structure.

By BiFc assay, the optineurin-optineurin interaction was directly visualized in the cytoplasm of Neuro2A cells (**Figure 6**). The dimer/oligomer formation is in agreement with previous findings of optineurin foci [12, 24], as well as high molecular weight complex formation and oligomerization demonstrated by gel filtration analysis, blue native gel electrophoresis, and an in situ proximity ligation assay [2, 12, 13]. Optineurin is in addition shown in the present study to be an aggregation prone protein as evidenced by ThT assay (**Figure 7**). ThT is a benzothiazole salt dye that is widely used to visualize and quantify the presence of amyloid aggregates, both in vitro and in vivo. When it binds to β sheet-rich amyloid fibril structures, the dye displays enhanced fluorescence and a characteristic red shift of its emission spectrum [55]. As shown in Figure 7A, increasing incubation time of purified optineurin protein in physiological condition led to an increased ThT fluorescence. Increasing ionic strength also increased the ThT fluorescence (**Figure 7B**). These indicate that optineurin can aggregate to form β sheet-rich fibril structures. Small aggregates were also observed by atomic force microscopy (AFM) after incubation at 4°C or 37°C in 50 mM Tris, 150 mM NaCl, pH 7.4 for 4 days (data not shown). Specific features or fibrils however were not seen. The experimental conditions for AFM might need to be further optimized. The AFM aggregates nevertheless may represent oligomer/multimer species of optineurin.

In neurodegenerative disorders, intracellular deposition of aggregated proteins into inclusion bodies, Lewy bodies, or aggresomes is a prominent cytopathological feature [56]. The sequestration of proteins (such as α -synuclein in Parkinson) into Lewy bodies or aggresomes is dependent on the microtubule-based pathway [57]. Similar to α -synuclein, optineurin is also demonstrated to be an aggregation prone protein. Foci formation by optineurin is contingent on the integrity of the microtubule network and overexpression of optineurin induces apoptosis [24, 58, 59]. These similarities further reinforce the association of optineurin with neurodegenerative diseases including glaucoma.

6. Conclusion

In the current study, mammalian expression of optineurin protein is demonstrated. Knowledge regarding its secondary structure, posttranslational modification sites and aggregation is attained. The biophysical information is of fundamental value and may help elucidate ultimately pathophysiological pathways triggered by optineurin mutants such as Glu⁵⁰ \rightarrow Lys (E50K) found in normal tension glaucoma [60] and Gln³⁹⁸ stop (Q398X) and Glu⁴⁷⁸ \rightarrow Gly (E478G) found in ALS [4].

7. List of Abbreviations

ALS, amyotrophic lateral sclerosis; BiFc, bimolecular fluorescence complementation; CD, circular dichroism; DAPI, 4',6-diamidino-2-phenylindole; Dox, doxycycline; EYFP, enhanced yellow fluorescent protein; GFP, green fluorescent protein; Halo-TEV, Halo-tagged TEV protease; LC-MS/MS, liquid chromatography-mass spectrometry; NEMO, NF- κ B essential molecule; NRP, NEMO related protein; OPTN, optineurin; OPTN-Halo, Halo tagged human wild type optineurin; Plk1, polo-like kinase 1; POAG, primary open angle glaucoma; TBK1, TANK (TRAF-associated NF- κ B activator) binding kinase 1; Tet-on, tetracycline inducible; ThT, thioflavin T; TNF- α , tumor necrosis factor- α ; UBD, ubiquitin-binding domain.

Acknowledgements

The authors thank Mr. Rod David from the Mass spectrometry, Metabolomics & Proteomics Facility, Research Resource Center at the University of Illinois at Chicago (UIC) for assistance in LC-MS/MS analysis; Dr. Gerd Prehna at the Center for Structural Biology, UIC, for assistance in CD measurements and analysis; Dr. Tao Xu from Department of Chemistry and Biochemistry, Northern Illinois University for assistance in AFM experiments; Dr. Tom Kerppola from University of Michigan for generously providing BiFc plasmids pbFos-YC and bJun-YN. We also thank Ms. Ruth Zelkha for assistance in imaging analysis and Mr. Dong-Jin Choi for technical assistance.

The work was supported in part by a grant from BrightFocus Foundation, Clarksburg, Maryland (B.Y.J.T.Y.), grant EY 018828 (B.Y.J.T.Y), core grant EY001792 from the National Eye Institute, Bethesda, Maryland, and an unrestricted departmental award from Research to Prevent Blindness, New York City, New York.

References

- [1] Li Y, Kang J, Horwitz MS. Interaction of an adenovirus E3 14.7-kilodalton protein with a novel tumor necrosis factor α -inducible cellular protein containing leucine zipper domains. *Mol Cell Biol.* 1998;18:1601-1610.
- [2] Schwamborn K, Weil R, Courtois G, Whiteside ST, Israel A. Phorbol esters and cytokines regulate the expression of the NEMO-related protein, a molecule involved in a NF- κ B-independent pathway. *J Biol Chem.* 2000;275:22780-22789.
- [3] Rezaie T, Child A, Hitchings R, Brice G, Miller L, Coca-Prados M, et al. Adult-onset primary open-angle glaucoma caused by mutations in optineurin. *Science.* 2002;295:1077-1079.
- [4] Maruyama H, Morino H, Ito H, Izumi Y, Kato H, Watanabe Y, et al. Mutations of optineurin in amyotrophic lateral sclerosis. *Nature.* 2010;465:223-226.
- [5] Maruyama H, Kawakami H. Optineurin and amyotrophic lateral sclerosis. *Geriatr Gerontol Int.* 2013;13:528-532.
- [6] Kamada M, Izumi Y, Ayaki T, Nakamura M, Kagawa S, Kudo E, et al. Clinicopathologic features of autosomal recessive amyotrophic lateral sclerosis associated with optineurin mutation. *Neuropathology.* 2014;34:64-70.
- [7] Rezaie T, Waitzman DM, Seeman JL, Kaufman PL, Sarfarazi M. Molecular cloning and expression profiling of optineurin in the rhesus monkey. *Invest Ophthalmol Vis Sci.* 2005;46:2404-2410.
- [8] Wild P, Farhan H, McEwan DG, Wagner S, Rogov VV, Brady NR, et al. Phosphorylation of the autophagy receptor optineurin restricts Salmonella growth. *Science.* 2011;333:228-233.
- [9] Hattula K, Peranen J (2000). FIP-2, a coiled-coil protein, links Huntingtin to Rab8 and modulates cellular morphogenesis. *Current Biology*, 10, 1603-1606.
- [10] Stroissnigg H, Repitz M, Miloloza A, Linhartova I, Beug H, Wiche G, Propst F. FIP-2, an I κ B-kinase- γ -related protein, is associated with the Golgi apparatus and translocates to the marginal band during chicken erythroblast differentiation. *Exp Cell Res.* 2002;278:133-145.
- [11] Ying H, Shen X, Yue BYJT. Establishment of inducible wild type and mutant myocilin-GFP-expressing RGC-5 cell lines. *PLoS One.* 2012;7:e47307.
- [12] Ying H, Shen X, Park B, Yue BYJT. Posttranslational modifications, localization, and protein interactions of optineurin, the product of a glaucoma gene. *PLoS One.* 2010;5:e9168.
- [13] Gao J, Ohtsubo M, Hotta Y, Minoshima S. Oligomerization of optineurin and its oxidative stress- or E50K mutation-driven covalent cross-linking: possible relationship with glaucoma pathology. *PLoS One.* 2014;9:e101206.
- [14] De Marco N, Buono M, Troise F, Diez-Roux G. Optineurin increases cell survival and translocates to the nucleus in a Rab8-dependent manner upon an apoptotic stimulus. *J Biol Chem.* 2006;281:16147-16156.

- [15] Chibalina MV, Roberts RC, Arden SD, Kendrick-Jones J, Buss F. Rab8-optineurin-myosin VI: analysis of interactions and functions in the secretory pathway. *Methods Enzymol.* 2008;438:11-24.
- [16] Del Toro D, Alberch J, Lazaro-Dieguez F, Martin-Ibanez R, Xifro X, Egea G, et al. Mutant huntingtin impairs post-Golgi trafficking to lysosomes by delocalizing optineurin/Rab8 complex from the Golgi apparatus. *Mol Biol Cell.* 2009;20:1478-1492.
- [17] Sahlender DA, Roberts RC, Arden SD, Spudich G, Taylor MJ, Luzio JP, et al. Optineurin links myosin VI to the Golgi complex and is involved in Golgi organization and exocytosis. *J Cell Biol.* 2005;169:285-295.
- [18] Park B, Ying H, Shen X, Park JS, Qiu Y, Shyam R, Yue BYJT. Impairment of protein trafficking upon overexpression and mutation of optineurin. *PLoS One.* 2010;5:e11547.
- [19] Nagabhushana A, Chalasani ML, Jain N, Radha V, Rangaraj N, Balasubramanian D, et al. Regulation of endocytic trafficking of transferrin receptor by optineurin and its impairment by a glaucoma-associated mutant. *BMC Cell Biol.* 2010;11:4.
- [20] Anborgh PH, Godin C, Pampillo M, Dhama GK, Dale LB, Cregan SP, et al. Inhibition of metabotropic glutamate receptor signaling by the huntingtin-binding protein optineurin. *J Biol Chem.* 2005;280:34840-34848.
- [21] Kachaner D, Filipe J, Laplantine E, Bauch A, Bennett KL, Superti-Furga G, et al. Plk1-dependent phosphorylation of optineurin provides a negative feedback mechanism for mitotic progression. *Mol Cell.* 2012;45:553-566.
- [22] Morton S, Hesson L, Pegg M, Cohen P. Enhanced binding of TBK1 by an optineurin mutant that causes a familial form of primary open angle glaucoma. *FEBS Lett.* 2008;582:997-1002.
- [23] Bond LM, Peden AA, Kendrick-Jones J, Sellers JR, Buss F. Myosin VI and its binding partner optineurin are involved in secretory vesicle fusion at the plasma membrane. *Mol Biol Cell.* 2011;22:54-65.
- [24] Park BC, Shen X, Samaraweera M, Yue BYJT. Studies of optineurin, a glaucoma gene: Golgi fragmentation and cell death from overexpression of wild-type and mutant optineurin in two ocular cell types. *Am J Pathol.* 2006;169:1976-1989.
- [25] Sippl C, Zeilbeck LF, Fuchshofer R, Tamm ER. Optineurin associates with the podocyte Golgi complex to maintain its structure. *Cell Tissue Res.* 2014;358:567-583.
- [26] Zhu G, Wu CJ, Zhao Y, Ashwell JD. Optineurin negatively regulates TNF α -induced NF- κ B activation by competing with NEMO for ubiquitinated RIP. *Curr Biol.* 2007;17:1438-1443.
- [27] Sudhakar C, Nagabhushana A, Jain N, Swarup G. NF- κ B mediates tumor necrosis factor α -induced expression of optineurin, a negative regulator of NF- κ B. *PLoS One.* 2009;4:e5114.
- [28] Mankouri J, Fragkoudis R, Richards KH, Wetherill LF, Harris M, Kohl A, et al. Optineurin negatively regulates the induction of IFN β in response to RNA virus infection. *PLoS Pathog.* 2010;6:e1000778.
- [29] Nagabhushana A, Bansal M, Swarup G. Optineurin is required for CYLD-dependent inhibition of TNF α -induced NF- κ B activation. *PLoS One.* 2011;6:e17477.
- [30] Akizuki M, Yamashita H, Uemura K, Maruyama H, Kawakami H, Ito H, et al. Optineurin suppression causes neuronal cell death via NF- κ B pathway. *J Neurochem.* 2013;126:699-704.
- [31] Shen X, Ying H, Qiu Y, Park JS, Shyam R, Chi ZL, et al. Processing of optineurin in neuronal cells. *J Biol Chem.* 2011;286:3618-3629.
- [32] Chalasani ML, Kumari A, Radha V, Swarup G. E50K-OPTN-induced retinal cell death involves the Rab GTPase-activating protein, TBC1D17 mediated block in autophagy. *PLoS One.* 2014;9:e95758.
- [33] Ying H, Yue BYJT. Optineurin: The autophagy connection. *Exp Eye Res.* 2015; epub ahead of print.
- [34] Rogov VV, Suzuki H, Fiskin E, Wild P, Kniss A, Rozenknop A, et al. Structural basis for phosphorylation-triggered autophagic clearance of Salmonella. *Biochem J.* 2013;454:459-466.
- [35] Kerppola TK. Bimolecular fluorescence complementation (BiFC) analysis of protein interactions in live cells. *Cold Spring Harb Protoc.* 2013:727-731.
- [36] Outeiro TF, Putcha P, Tetzlaff JE, Spoelgen R, Koker M, et al. Formation of toxic oligomeric α -synuclein species in living cells. *PLoS One.* 2008;3:e1867.
- [37] Ying H, Yue BYJT. Cellular and molecular biology of optineurin. *Int Rev Cell Mol Biol.* 2012;294:223-258.

- [38] Hu CD, Chinenov Y, Kerppola TK. Visualization of interactions among bZIP and Rel family proteins in living cells using bimolecular fluorescence complementation. *Mol Cell*. 2002;9:789-798.
- [39] Whitmore L, Wallace BA. DICHROWEB, an online server for protein secondary structure analyses from circular dichroism spectroscopic data. *Nucleic Acids Res*. 2004;2:W668-W673.
- [40] Whitmore L, Wallace BA. Protein secondary structure analyses from circular dichroism spectroscopy: Methods and reference databases. *Biopolymers*. 2008;89:392-400.
- [41] Osawa T, Mizuno Y, Fujita Y, Takatama M, Nakazato Y, Okamoto K. Optineurin in neurodegenerative diseases. *Neuropathology*. 2011;31:569-574.
- [42] Schwab C, Yu S, McGeer EG, McGeer PL. Optineurin in Huntington's disease intranuclear inclusions. *Neurosci Lett*. 2012;506:149-154.
- [43] Fuse N, Takahashi K, Akiyama H, Nakazawa T, Seimiya M, Kuwahara S, et al. Molecular genetic analysis of optineurin gene for primary open-angle and normal tension glaucoma in the Japanese population. *J Glaucoma*. 2004;13:299-303.
- [44] Liu YH, Tian T. Hypothesis of optineurin as a new common risk factor in normal-tension glaucoma and Alzheimer's disease. *Med Hypotheses*. 2011;77:591-592.
- [45] Ito H, Nakamura M, Komure O, Ayaki T, Wate R, Maruyama H, et al. Clinicopathologic study on an ALS family with a heterozygous E478G optineurin mutation. *Acta Neuropathol*. 2011;122:223-229.
- [46] Ito H, Fujita K, Nakamura M, Wate R, Kaneko S, Sasaki S, et al. Optineurin is co-localized with FUS in basophilic inclusions of ALS with FUS mutation and in basophilic inclusion body disease. *Acta Neuropathol*. 2011;121:555-557.
- [47] Van Bergen NJ, Wood JP, Chidlow G, Trounce IA, Casson RJ, Ju WK, et al. Recharacterization of the RGC-5 retinal ganglion cell line. *Invest Ophthalmol Vis Sci*. 2009;50:4267-4272.
- [48] Krishnamoorthy RR, Clark AF, Daudt D, Vishwanatha JK, Yorio T. A forensic path to RGC-5 cell line identification: lessons learned. *Invest Ophthalmol Vis Sci*. 2013;54:5712-5719.
- [49] Sippl C, Tamm ER. What is the nature of the RGC-5 cell line? *Adv Exp Med Biol*. 2014;801:145-154.
- [50] Ohana RF, Hurst R, Vidugiriene J, Slater MR, Wood KV, Urh M. HaloTag-based purification of functional human kinases from mammalian cells. *Protein Expr Purif*. 2011;76:154-164.
- [51] Archambault V, Glover DM. Polo-like kinases: conservation and divergence in their functions and regulation. *Nat Rev Mol Cell Biol*. 2009;10:265-275.
- [52] Helgason E, Phung QT, Dueber EC. Recent insights into the complexity of Tank-binding kinase 1 signaling networks: the emerging role of cellular localization in the activation and substrate specificity of TBK1. *FEBS Lett*. 2013;587:1230-1237.
- [53] Korac J, Schaeffer V, Kovacevic I, Clement AM, Jungblut B, Behl C, et al. Ubiquitin-independent function of optineurin in autophagic clearance of protein aggregates. *J Cell Sci*. 2013;126:580-592.
- [54] Starheim KK, Gevaert K, Arnesen T. Protein N-terminal acetyltransferases: when the start matters. *Trends Biochem Sci*. 2012;37:152-161.
- [55] LeVine H 3rd. Quantification of β -sheet amyloid fibril structures with thioflavin T. *Methods Enzymol*. 1999;309:274-284.
- [56] Chhangani D, Mishra A. Protein quality control system in neurodegeneration: a healing company hard to beat but failure is fatal. *Mol Neurobiol*. 2013;48:141-156.
- [57] Johnston JA, Illing ME, Kopito RR. Cytoplasmic dynein/dynactin mediates the assembly of aggresomes. *Cell Motil Cytoskeleton*. 2002;53:26-38.
- [58] Koga T, Shen X, Park JS, Qiu Y, Park BC, Shyam R, et al. Differential effects of myocilin and optineurin, two glaucoma genes, on neurite outgrowth. *Am J Pathol*. 2010;176:343-352.
- [59] Ying H, Turturro S, Nguyen T, Shen X, Zelkha R, Johnson EC, et al. Induction of autophagy in rats upon overexpression of wild-type and mutant optineurin gene. *BMC Cell Biol*. 2015;16:14.
- [60] Aung T, Rezaie T, Okada K, Viswanathan AC, Child AH, Brice G, et al. Clinical features and course of patients with glaucoma with the E50K mutation in the optineurin gene. *Invest Ophthalmol Vis Sci*. 2005;46:2816-2822.